Applied Catalysis B: Environmental 199 (2016) 45–54

Contents lists available at ScienceDirect

Applied Catalysis B: Environmental

journal homepage: www.elsevier.com/locate/apcatb

Toluene oxidation over ZrO_2-based gasification gas clean-up catalysts: Part B. Kinetic modeling

Tiia Viinikainen*, Sonja Kouva, Juha Lehtonen, Jaana Kanervo

Aalto University, School of Chemical Technology, Department of Biotechnology and Chemical Technology, P.O. Box 16100, 00076 Aalto, Finland

ARTICLE INFO

Article history:
Received 8 February 2016
Received in revised form 2 June 2016
Accepted 4 June 2016
Available online 8 June 2016

Keywords:
Zirconia
Toluene oxidation
Temperature-programmed surface reaction
Kinetic modeling
Gasification gas cleaning

ABSTRACT

Energy, liquid biofuels and chemicals can be produced from biomass via gasification followed by gas cleaning over ZrO_2-based catalysts. When a small amount of oxygen is added, ZrO_2-based catalysts can be utilized in tar decomposition reactions (tar molecules need to be removed before further use). Oxidation of toluene as tar model compound was studied by temperature-programmed experiments over ZrO_2, Y_2O_3-ZrO_2 and SiO_2-ZrO_2. In the first part of this study (Part A: Effect of oxygen on the formation of primary products), special attention was given to the effect of oxygen amount on the formation of synthesis gas components (CO and H_2) from toluene. The data obtained in Part A was extended and subjected to kinetic modeling. As a result, the reaction mechanism of toluene oxidation over ZrO_2-based catalysts was discovered. The first step in toluene oxidation is the adsorption of toluene as a benzyl species. Next, the surface benzyl species is oxidized, possibly *via* superoxide surface species (O_2^-), into four products in a single net primary reaction. Oxidation of CO and H_2 are the secondary reactions in the model. Furthermore, the present study clearly demonstrates the strength of temperature programming as a transient technique for comprehensive mechanistic investigations, kinetic model development and parameter estimation.

1. Introduction

Biomass gasification is an environmentally appealing way to produce heat and power, liquid biofuels and various chemicals [1]. The gas from biomass gasification contains impurities, such as tar (aromatic hydrocarbons heavier than benzene), and thus it has to be cleaned before use [2]. A catalytic hot gas cleaning unit after the gasifier is one of the most advantageous technologies to decompose the tar molecules [3,4]. Therefore, the activities of several catalysts have been screened in catalytic hot gas cleaning. Typically, dolomite ($MgCO_3$·$CaCO_3$), alkali metal and nickel catalysts have been used in tar reforming [2]. Moreover, ZrO_2-based catalysts have shown to selectively oxidize tar molecules into CO_2 and CO in biomass gasification gas when a small amount of oxygen is added to the gas (e.g. [5–7]). In order to optimize the gas cleaning catalyst and to enable process design ensuring a high-quality product gas, detailed knowledge of tar decomposition mechanisms needs to established.

In our previous contributions, toluene adsorption and oxidation over ZrO_2-based catalysts have been studied by in situ DRIFTS (diffuse reflectance infrared Fourier transform spectroscopy) and temperature-programmed experiments [8,9]. These experiments indicated toluene oxidation activity between 300 and 600 °C and the results implied that the key intermediate in toluene oxidation is a surface benzyl species [8,9]. Furthermore, toluene was shown to be oxidized into four products: CO_2, CO, H_2O and H_2 [9]. Toluene was completely consumed at 600 °C over all catalysts but the conversion of oxygen was not complete (80–90% at 600 °C) [9]. The formation of CO and H_2 was detected over pure ZrO_2 even with the highest feed ratio (≈3.5 × theoretical toluene total oxidation ratio) at 600 °C, whereas over the doped zirconias (Y_2O_3-ZrO_2 and SiO_2-ZrO_2) the formation of CO and H_2 approached zero above 550 °C when over-stoichiometric O_2-toluene ratios were used. As a continuation for these publications, this work addresses the oxidation kinetics of toluene over ZrO_2-based gasification gas clean-up catalysts.

Toluene oxidation kinetics has been studied lately in the field of VOC (volatile organic compounds) abatement over several transition metal oxide catalysts (e.g. [10,11]). However, the kinetic models obtained in VOC oxidation studies cannot be directly applied to gasification gas cleaning since the main goals of these two fields differ. In gasification gas cleaning the aim is to convert tar molecules into valuable gas components (such as CO and H_2) [4], while in VOC abatement the goal is the complete oxidation of VOC solely into CO_2 and H_2O [12]. Since our earlier works [8,9] have

* Corresponding author.
E-mail address: tiia.viinikainen@aalto.fi (T. Viinikainen).

http://dx.doi.org/10.1016/j.apcatb.2016.06.015
0926-3373/

Table 1
Experiments applied in kinetic modeling of toluene oxidation.

Catalyst	O_2-toluene feed ratio (mol/mol)	Heating rate (°C)	Reference
ZrO_2	9.9 (≈1.1 × theoretical ratio)	6.7 and 15	Present work
ZrO_2	9.9 (≈1.1 × theoretical ratio)	10	[9]
ZrO_2	18.2 (≈2.0 × theoretical ratio)	10	[9]
ZrO_2	31.2 (≈3.5 × theoretical ratio)	10	[9]
Y_2O_3-ZrO_2	9.9 (≈1.1 × theoretical ratio)	6.7 and 15	Present work
Y_2O_3-ZrO_2	9.9 (≈1.1 × theoretical ratio)	10	[9]
Y_2O_3-ZrO_2	18.2 (≈2.0 × theoretical ratio)	10	[9]
Y_2O_3-ZrO_2	31.2 (≈3.5 × theoretical ratio)	10	[9]
SiO_2-ZrO_2	9.9 (≈1.1 × theoretical ratio)	6.7 and 15	Present work
SiO_2-ZrO_2	9.9 (≈1.1 × theoretical ratio)	10	[9]
SiO_2-ZrO_2	18.2 (≈2.0 × theoretical ratio)	10	[9]
SiO_2-ZrO_2	31.2 (≈3.5 × theoretical ratio)	10	[9]

showed the formation of two additional products, i.e., CO and H_2, the kinetic model of toluene oxidation over ZrO_2-based gasification gas clean-up catalysts must explain the formation of CO and H_2 as well.

Temperature-programmed (TP) experiments provide predictions for the reaction rates under dynamic conditions and allows multiscale reaction modeling [13]. Additionally, when applying the temperature-programmed techniques, data for kinetic modeling can be collected with a moderate number of experiments, thus considerably accelerating the work of catalyst testing [14,15]. Three different modes of temperature-programmed techniques have been applied for kinetic modeling: the desorption of an adsorbed component (TPD, e.g. [13,16]), determination of the catalyst reducibility (TPR, e.g. [17,18]) or coke oxidation from the catalyst surface (TPO, e.g. [19,20]). Typically, in temperature-programmed surface reactions (TPSR) one reactant is pre-adsorbed on the catalyst and the other reactant is fed while increasing the temperature. In our case the pre-adsorption of one reactant is not adequate, because the formation of the reactive intermediate (surface benzyl species) is an activated process according to our previous findings [8]. Therefore, co-feeding of toluene and oxygen during temperature-programmed heating was carried out.

The aim of this work is to determine the reaction kinetics of toluene oxidation by applying transient conditions (temperature-programming) in an atmospheric flow-through TP setup, and to relate the kinetics to relevant elementary surface reaction steps in toluene oxidation over ZrO_2-based gasification gas clean-up catalysts. Furthermore, this study will demonstrate the applicability of co-feeding type temperature-programmed reaction experiment for kinetic determinations.

2. Experimental

2.1. Toluene oxidation experiments

ZrO_2-based powder samples (pure ZrO_2, 5 mol-% Y_2O_3-ZrO_2 and 8 mol-% SiO_2-ZrO_2), supplied by MEL Chemicals, were calcined at 800 °C for 1 h in static air. The physical and chemical characteristics of the catalysts have been reported elsewhere [7,8,21]. The calcined catalysts were pressed into pellets, crushed and sieved to the particle size of 0.25–0.42 mm.

The kinetic data was collected in an Altamira AMI–200 R catalyst characterization system attached to an on-line mass spectrometer (Hiden QIC-20). The experiments published in [9] were accompanied with toluene oxidation experiments applying different heating rates over ZrO_2-based catalysts. The dehydroxylation of the ZrO_2 surface was studied in toluene adsorption experiment.

The same procedure was applied in all experiments: calcination at 600 °C for 2 h (in 5 vol-% O_2/He), cooling down to 200 °C (in 2.5 vol-% O_2/He), helium flush for 1 h, stabilization under the reaction mixture for 2 h at 200 °C, heating up to 600 °C (10 °C/min) and stabilization for 30 min at 600 °C under the reaction mixture. The total gas flow rate was kept at 50 cm^3/min. Typically 100 mg of sample was used.

In toluene oxidation experiments, the reaction mixture was achieved by mixing toluene (685 ppm toluene in He with ca. 260 ppm water as impurity) with oxygen (5 vol-% in He). Three heating rates of 6.7, 10 and 15 °C/min were applied. All the experiments applied in kinetic modeling of toluene oxidation have been collected into Table 1. In the toluene adsorption experiment over ZrO_2, the reaction mixture consisted of toluene in He. The heating rate of 10 °C/min was used.

Mass spectrometry was used to analyze the composition of the gas flow at the outlet of the reactor in all the experiments. Signals with mass-to-charge ratios of 2 (H_2), 15 (CH_4), 18 (H_2O), 28 (CO), 32 (O_2), 44 (CO_2), 78 (benzene) and 91 (toluene) were followed. A single-point calibration was used to quantify the molar amounts of toluene and oxygen from the feed. A single-point calibration for water with a calibration gas (0.09 vol-% H_2O/He) was applied. To obtain fully closed mass balances at the steady state (at 600 °C) of the experiments, the calibration factors for CO_2, CO and H_2 (and an adjusted one for H_2O) were calculated.

2.2. Kinetic modeling

The kinetic parameters were estimated using nonlinear regression by minimizing the sum of squared residuals between the measured and the modeled molar flows of reaction components:

$$\sum_{i=1}^{n}\sum_{j=1}^{N}\left(F_{i,exp,j}-F_{i,calc,j}\right)^2 \quad ,(1)$$

where $F_{i,exp,j}$ is the measured molar flow of gas-phase component i at data point j, $F_{i,calc,j}$ is the calculated molar flow of gas phase component i at data point j, n is the number of gas-phase species and N is the number of data points.

The reactor was modeled as a dynamic pseudohomogeneous plug flow reactor, which is applicable as intraparticle mass transfer can be excluded and molar flows have a gradient in the axial direction [22]:

$$\frac{dc_i}{dt}=-\frac{U(t)}{L\varepsilon_b}\frac{dc_i}{dx}+\frac{(1-\varepsilon_b)}{\varepsilon_b}\rho_p r'_i \quad ,(2)$$

where c_i is the gas phase concentration of gas phase component i (μmol/cm^3), t is time (s), U is the superficial velocity (cm/s), L is the length of catalyst bed (cm), ε_b is the porosity of the catalyst bed (−), x is the dimensionless coordinate of the catalyst bed (−), ρ_p is the density of catalyst particles (g_{cat}/cm^3) and r'_i is the reaction rate of gas-phase component i (μmol/[g_{cat} s]). Although the studied reaction is highly exothermic, the catalyst temperature was considered to be uniform with the gas phase in these experiments as the feed consisted mostly of inert gas (He > 98 vol-%), which was

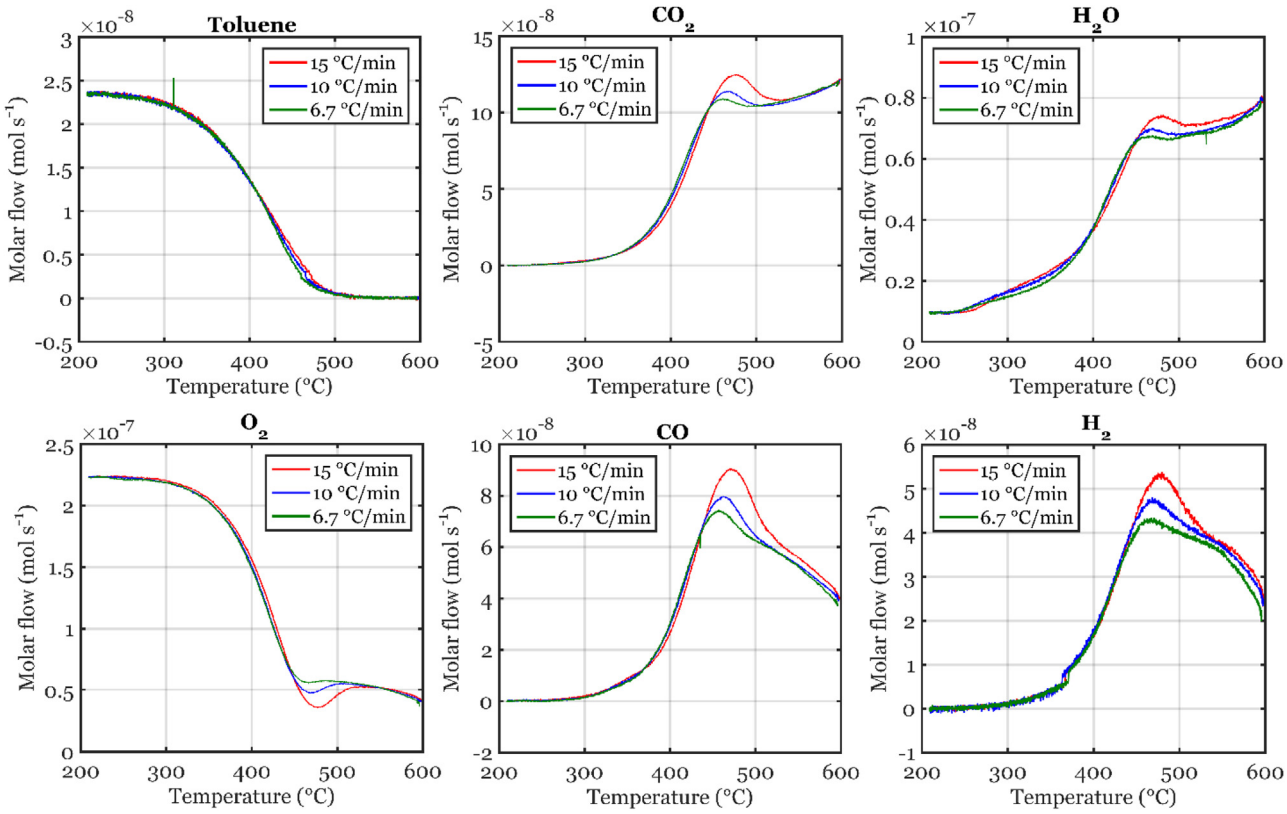

Fig. 1. TPSR profiles of the components at the reactor outlet with heating rates of 6.7, 10 and 15 °C/min over ZrO_2.

estimated to be able to maintain isothermal conditions inside the reactor. The temperature measurement right after the catalyst bed did not indicate any fluctuation from the linear trend in the course of experiment.

The temperature dependency of all reaction rate constants was taken into account using the reparametrized Arrhenius equation:

$$k = k_{ref} exp\left[\frac{E_A}{R}\left(\frac{1}{T_{ref}} - \frac{1}{T}\right)\right] \quad , (3)$$

where k_{ref} is the rate constant of a reaction at reference temperature (−), E_A is the activation energy of a reaction (kJ/mol), R is the universal gas constant (J/[mol K]), T_{ref} is the representative reference temperature (688 K) and T is temperature (K).

The parameters to be estimated were then k_{ref} and E_A of all the reactions. In order to convert the PDE system of reactor mass balances to an ODE system and to solve the spatial derivatives, the axial coordinate (x) of the catalyst bed was discretized non-equidistantly: the 20 discretization points along the catalyst bed were placed more densely at the beginning of the bed. The ODE equations were solved using the ODE15s routine and parameter values were optimized applying a bounded optimization package FMINSEARCBND [23] in MATLAB® R2015a.

3. Results and discussion

Several temperature-programmed experiments were performed in order to obtain mechanistic insight into toluene oxidation and the possible secondary reactions. The obtained data from the first part of this study [9] was complemented with experiments applying multiple heating rates. The obtained extensive data was analyzed thoroughly and a kinetic model for toluene oxidation was postulated. The kinetic model was tested against all the measured molar flows (toluene, O_2, CO_2, H_2O, CO and H_2) of the temperature-programmed toluene oxidation experiments.

3.1. Effect of heating rate

Toluene oxidation TPSR profiles of the components at the reactor outlet with three heating rates over ZrO_2 are shown in Fig. 1. Toluene was completely consumed above 500 °C in all experiments. In contrast, oxygen was not fully consumed even at 600 °C, in agreement with the limiting reactant being toluene. Based on our prior results [9], only CO_2, H_2O, CO and H_2 were formed, as expected. The fact that no other products were observed gives valuable mechanistic insight into toluene oxidation over these catalysts. The formation of CO_2 and H_2O increased with increasing temperature throughout the studied temperature range whereas the formation of CO and H_2 first increased with increasing temperature and then started to decrease at ca. 480 °C.

The TPSR profiles of the products over ZrO_2 depict the effect of the heating rate elegantly; with increasing heating rate the maxima shift to higher temperatures and the sharpness of the profiles increases [24]. Likewise, the increase in the intensity of the profiles is approximately proportional to the heating rate. A shoulder at ca. 550 °C in the profiles of CO and H_2 starts to distinguish more clearly with a lower heating rate.

Over the doped catalysts (Figs. S1 and S2 in the Supplementary data), the increase in the heating rate shifted the maxima to higher temperatures and the sharpness of the TPSR profiles increased similarly to pure ZrO_2. Over Y_2O_3-ZrO_2 (Fig. S1 in the Supplementary data), the profiles of CO and H_2 also showed more distinguishable shoulders at 550 °C with a lower heating rate. However, changing the heating rate over SiO_2-ZrO_2 (Fig. S2 in the Supplementary data) did not add any new features to the profiles.

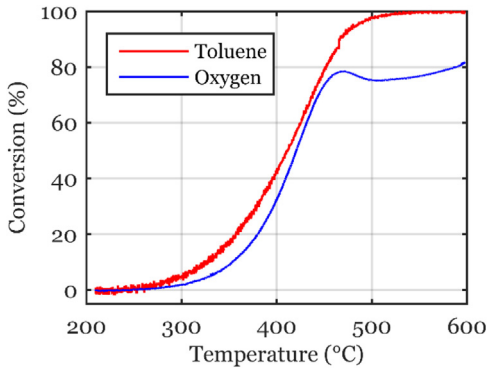

Fig. 2. Comparison of toluene and oxygen conversion over ZrO_2 (heating rate: 10 °C/min).

3.2. Data analysis

A careful analysis of temperature-programmed toluene oxidation experiments over ZrO_2-based catalysts illustrated several characteristics that can be applied in the derivation of surface reaction mechanisms. First of all, the conversion of oxygen started at slightly higher temperatures than the conversion of toluene (shown for ZrO_2 in Fig. 2) suggesting that adsorbed surface species originating from toluene are involved in the reactions. In addition, different dynamics in toluene and oxygen conversions, the latter manifesting a local maximum around 460 °C, imply that oxygen is being converted in a subsequent reaction unrelated to the primary toluene conversion. In order to draw further conclusions on the nature of the surface species, dehydroxylation of the surface was excluded from the results. The dehydroxylation of the ZrO_2 surface was studied in a separate experiment, where toluene was fed on ZrO_2 without oxygen while heating from 200 °C to 600 °C. A small amount of water was formed between 250 °C and 600 °C, with a maximum at 350 °C. This desorbed water signal was then subtracted from the water signal in toluene oxidation for the calculation of correct C, O and H atom consumptions and formations related to toluene oxidation (Fig. 3).

The consumption and formation of C, H and O atoms are shown in Fig. 3. It can be seen from the temperature range of 200–400 °C that when toluene oxidation is initiated, the consumption of both C and H atoms exceeds their formation. In the case of O atoms, such a difference in the consumption and formation curves cannot be observed. Thus, it seems that the intermediate surface species consist mainly of carbon and hydrogen. Separate surface spectroscopy studies [8] did not identify any other surface species than a surface benzyl species relevant for the reaction on these catalysts. The formation of surface benzyl species was detected only in the presence of gas phase oxygen [8]. Therefore, it is suggested that toluene first adsorbs as a surface benzyl species (reaction R1) that will then react further. The abstracted H atom in Reaction (R1) could retain as a surface hydroxyl (mOH) or evolve into gas phase in association with other species. The abstracted hydrogen is tentatively described to be desorbed directly into the gas phase in the model but this will be re-evaluated if necessary.

$$C_7H_8(g) \rightarrow [C_7H_7] + [H] \quad (R1)$$

The TPSR profiles (Fig. 4) of the products show two shapes; CO_2 and H_2O profiles resemble one another and CO and H_2 profiles are pairwise similar as well over each catalyst. The formation of CO_2 and H_2O increased with increasing temperature over all the catalysts. The formation of CO and H_2 first increased with increasing temperature and then started to decrease over all the catalysts at ca. 450–480 °C. Shape similarity of the products has been observed over Y_2O_3-ZrO_2 in the partial oxidation of methane by Zhu et al. [25]. The shape of CO_2 and H_2O formation curves were similar to each other and those of CO and H_2 were alike suggesting that products were formed in pairs in methane oxidation [25]. However, in methane oxidation over Y_2O_3-ZrO_2 the formation of CO and H_2 increased with increasing temperature (from 500 °C to 1100 °C) [25], while in toluene oxidation (present work) their formation first increased and then started to decrease with increasing temperature (from 200 °C to 600 °C). Another interesting similarity in product formation shapes was reported by Schmidt et al. [26] in temperature-programmed oxidation of naphthalene (as a tar model compound) over a Mo/V/W catalyst, the product formation curve shapes obtained for CO_2 and H_2O were similar to those over ZrO_2 (present work). Also the consumption curves of naphthalene and oxygen over the Mo/V/W catalyst showed a remarkable similarity to the consumption curves of toluene and oxygen over ZrO_2-based catalysts. In addition, Schmidt et al. [26] reported that in the presence of hydrogen and carbon monoxide naphthalene was fully converted at 500 °C with negligible conversions of CO and H_2, yet the possible formation of these two was not reported.

In addition to the main shapes of TPSR curves, small unique features can be observed over each catalyst (Fig. 4). Over pure ZrO_2, the formation of water started at slightly lower temperatures than the formation of other products. This formation of water is related to the dehydroxylation of the ZrO_2 surface as discussed above. A small shoulder in the water formation curves at 350 °C can be detected also over the doped catalysts. It has been reported by Kogler et al.

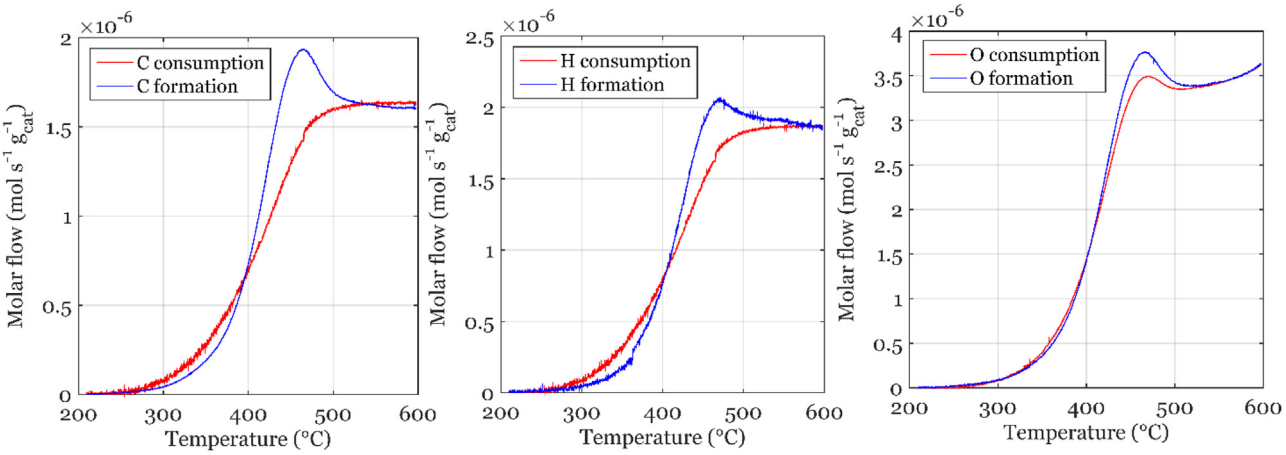

Fig. 3. The consumption and formation of C, H and O atoms in toluene oxidation over ZrO_2.

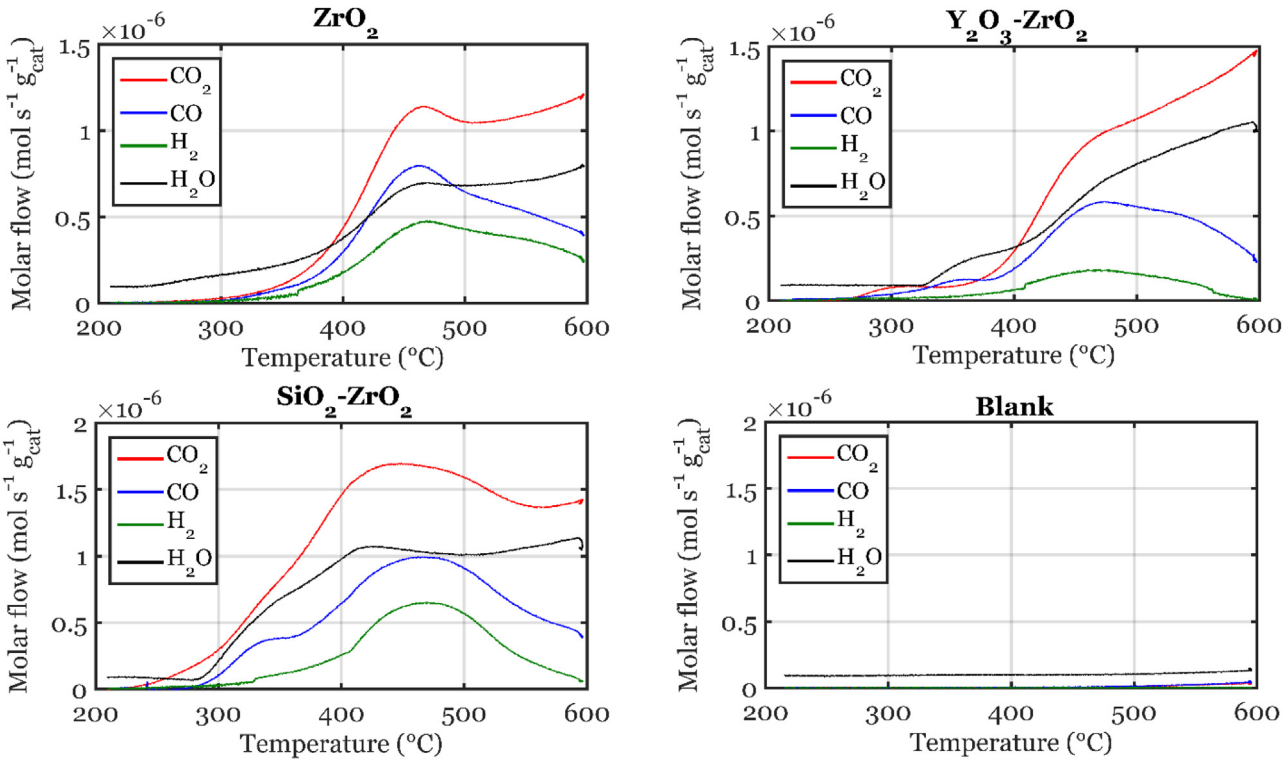

Fig. 4. The TPSR profiles of products in the temperature-programmed oxidation of toluene over ZrO_2-based catalysts and without catalyst (blank), heating rate: 10 °C/min.

[27] that over Y_2O_3-ZrO_2 water desorption can be observed even after reduction and evacuation. The water desorption is related to the dehydroxylation of the Y_2O_3-ZrO_2 surface. Therefore, it is suggested that the water evolution at lower temperatures is due to the dehydroxylation of the catalyst surfaces over all the ZrO_2-based catalysts.

Over the doped catalysts, additional evolution of carbon oxides can be seen from the shoulders of the curves. The formation curve of CO_2 over Y_2O_3-ZrO_2 shows a shoulder around 300 °C. Also in the formation curve of CO a shoulder can be seen around 350 °C over both doped catalysts. The origin of CO_2 and CO desorption from the surface could be explained by decomposition of formate and carbonate species resulting from minor toluene oxidation activity over the doped catalysts already at 200 °C. The data of pure ZrO_2 was chosen for kinetic modeling as over this catalyst only a small amount of water desorbed (dehydroxylation) and no desorption of carbon oxides was observed before toluene oxidation.

Recalling the paired formation of the products (Fig. 4), it is suggested that CO_2 and H_2O are mainly produced in the same reaction, therefore the ratio of CO_2 and H_2O (shown for pure ZrO_2 in Fig. 5) was calculated. Interestingly, a rather steady ratio (ca. 2) was obtained at the temperature range of 300–500 °C. Therefore the formation intermediate of CO_2 and H_2O must have a structure of $[C_xH_x]$. The fact that not even trace amounts of other aromatics or their partially oxygenated products were formed indicates that the next reaction step after toluene adsorption as benzyl species (R1) must include the disassembly of the benzene ring. In the most simplified model, the paired formation of CO_2 and H_2O could be due to the direct oxidation of the surface benzyl species.

In a similar manner, the ratio of CO and H_2 was calculated (shown for pure ZrO_2 in Fig. 5). This ratio is nearly as steady as CO_2/H_2O ratio. It probably shows a slight retaining/release processes of formed CO species at temperatures below 450 °C. The CO/H_2 ratio slightly increases with increasing temperature above 335 °C, implying that more CO is formed than H_2. The minor deviation in the formation and consumption of O atoms (on the right in Fig. 3) suggests that a small amount of CO desorbs from the catalyst surface at this point. Also, if the abstracted H atom is cleaved upon benzyl formation from toluene, rationalizing the CO/H_2 formation ratio is less straightforward. Nonetheless, the CO/H_2 ratio ranges between 1.5 and 1.8.

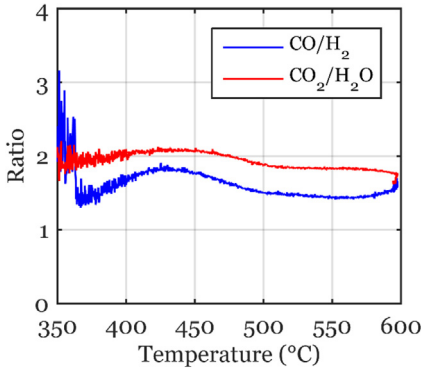

Fig. 5. CO_2/H_2O and CO/H_2 ratios over pure ZrO_2.

In addition to the stable CO_2/H_2O ratio, the ratio of CO_2/CO was reported in the first part of this study [9] to be likewise rather constant (≈1.3) up to 450 °C. This ratio is achieved when seven carbon atoms of the benzyl species react so that 4 CO_2 molecules and 3 CO molecules are formed. All of the obtained product ratios are met when the surface benzyl species react in a net Reaction (R2).

$$[C_7H_7] + 6.5O_2(g) \rightarrow 4CO_2(g) + 3CO(g) + 2H_2O(g) + 1.5H_2(g) \quad \text{(R2)}$$

It was shown in Part A [9], that in a separate CO oxidation experiment all the ZrO_2-based catalysts possessed activity towards CO oxidation. Therefore, it is proposed that surface-catalyzed CO oxi-

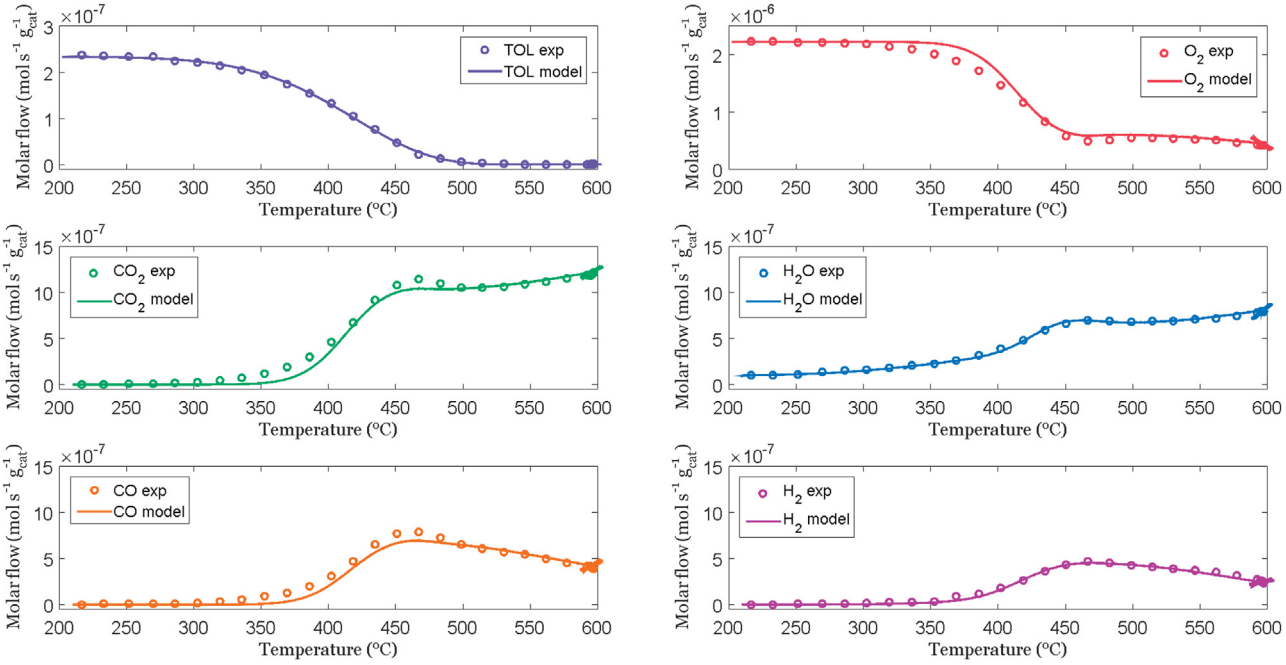

Fig. 6. Comparison between experimental data (open circles) and calculated molar flows (solid line) over pure ZrO_2 (O_2-toluene feed ratio: 1.1 × theoretical toluene total oxidation ratio, heating rate: 10 °C/min).

dation (Reaction (R3)) is a secondary reaction in toluene oxidation. Keeping in mind the shape similarity of CO and H_2 formation curves, the surface-catalyzed oxidation of H_2 (Reaction (R4)) was suggested to be a secondary reaction as well.

$$CO(g) + 0.5O_2(g) \rightarrow CO_2(g) \quad (R3)$$

$$H_2(g) + 0.5O_2(g) \rightarrow H_2O(g) \quad (R4)$$

The dehydroxylation of the ZrO_2 surface is taken into account by a reaction, where two hydroxyl groups are combined to yield water (Reaction (R5)) similar to the postulation of Bianchi et al. [28] reported in methanol TPD over ZrO_2. The reverse reaction (Reaction (R6)) was included since water (being a minor impurity in toluene/He mixture) entering the system caused additional hydroxylation of ZrO_2 surface in accordance with our previous findings in toluene TPD experiments [8]. The (de)hydroxylation reactions (Reactions (R5) and (R6)) presented here are simplified, whereas a more detailed illustration of the (de)hydroxylation mechanism over ZrO_2 surface has recently been published by Kouva et al. [29].

$$2Zr\text{-}OH \rightarrow H_2O(g) + Zr\text{-}O\text{-}Zr \quad (R5)$$

$$Zr\text{-}O\text{-}Zr + H_2O(g) \rightarrow 2Zr\text{-}OH \quad (R6)$$

3.3. Kinetic modeling

All toluene oxidation experiments (three heating rates and three feed ratios) measured in the temperature range of 200–600 °C were used in kinetic modeling. Kinetic parameters of the model were estimated by nonlinear regression by minimizing the sum of squared residuals between the measured and modeled molar flows of the reaction components (Eq. (1)). The reactor was modeled as a dynamic pseudohomogeneous plug flow reactor (Eq. (2)). The initial amounts of Zr-OH and Zr-O-Zr surface sites available for toluene oxidation were included in the parameter estimations.

The kinetic model consisting of Reactions (R1)–(R6) was tested via model fitting against the temperature-programmed toluene oxidation experiments with three different heating rates. The calculated and experimental molar flows of each component are shown in Fig. 6 for pure ZrO_2. For the sake of clarity, only every 50th experimental data point is shown. The multiple overlapping experimental data points (open circles) at the end of the ramp with all the components are the ones measured during the 30 min hold at 600 °C. This steady state was included in the modeling.

It can be seen from Fig. 6 that the molar flows of all hydrogen-containing components (toluene, water and hydrogen) were predicted extremely well with the model ($R^2 = 0.987$), whereas the molar flows of the other components were predicted adequately. However, the model was capable of producing the shapes of all TPSR curves at nearly correct temperatures and especially the overlapping data points at the steady state (at 600 °C). Small deviation was seen in the experimental and calculated molar flows of oxygen in the temperature range from 325 °C to 425 °C where the model slightly overestimated the oxygen molar flow, i.e., the true consumption of oxygen was slightly underestimated. Likewise, the model slightly underestimated the CO_2 and CO flows at their maxima and the calculated molar flows of these two started to increase at slightly higher temperatures than the experimental ones.

The parameters obtained with the model over pure ZrO_2 are collected in Table 2. The first step in the model (Reaction (R1)), namely the formation of surface benzyl species, has an activation energy of 88 kJ/mol. However, the most activated step is the net oxidation reaction of the surface benzyl species into the four products (R2) having activation energy of 179 kJ/mol. To the best of our knowledge, the only toluene oxidation kinetic study that included pure ZrO_2 (in a study of Mo oxides on different supports) has been published by Nag et al. [30]. The oxidation and reduction steps over pure ZrO_2 were reported to have activation energies of 121 kJ/mol and 49 kJ/mol, respectively [30]. Activation energies over other catalysts than ZrO_2 have been reported to range from 82.86 kJ/mol to 109.0 kJ/mol [11,31,32] assuming Langmuir-Hinshelwood kinetics and dissociative adsorption of oxygen. When LH-type model was considered with associative adsorption of oxygen, activation energy of 125.0 kJ/mol was obtained over $LaFeO_3$ catalyst [33].

The activation energies in the present work obtained for CO and H_2 oxidation are 97 and 113 kJ/mol, respectively. It is possible that consecutive oxidation reactions of CO and H_2 actually proceed from

Table 2
The model (R^2 = 0.992) parameters obtained over ZrO_2.

Reaction		Pre-exponential factor	Activation energy (kJ/mol)	k_{ref} (T_{ref} = 688 K)
(R1)	C_7H_8 (g) → [C_7H_7] + 0.5H_2 (g)	4.3×10^7	88	9.2 cm^3/s
(R2)	[C_7H_7] + 6.5O_2 → 4CO_2 (g) + 3CO (g) + 2H_2O (g) + 1.5H_2 (g)	2.6×10^{17}	179	6.6×10^3 cm^3/(s μmol)
(R3)	CO (g) + 0.5O_2 (g) → CO_2 (g)	1.8×10^{13}	97	7.3×10^5 cm^3/(s μmol)
(R4)	H_2 (g) + 0.5O_2 (g) → H_2O (g)	2.0×10^{14}	113	5.8×10^5 cm^3/(s μmol)
(R5)	2Zr-OH → H_2O (g) + Zr-O-Zr	3.1×10^7	111	0.1 cm^3/s
(R6)	Zr-O-Zr + H_2O (g) → 2Zr-OH	1.3×10^6	0	1.3×10^6 cm^3/(s μmol)

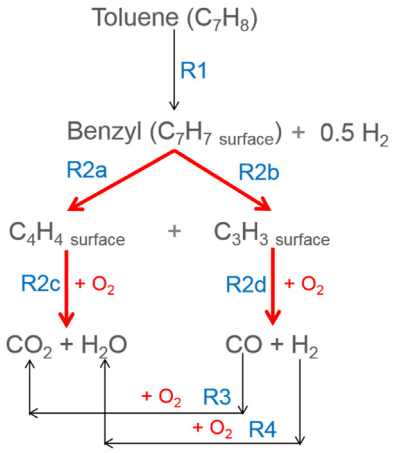

Fig. 7. Schematic presentation of the derived model. Reaction steps with red arrows have been lumped as one Reaction (R2). (For interpretation of the references to colour in this figure legend, the reader is referred to the web version of this article.)

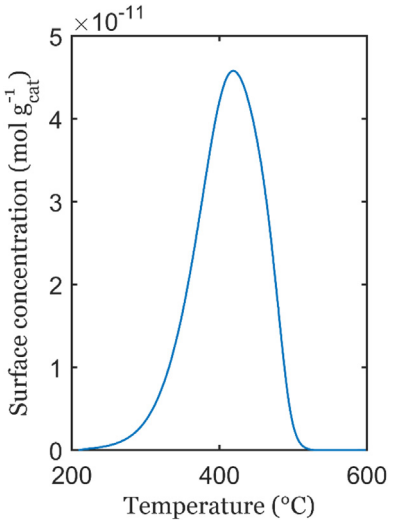

Fig. 8. Calculated concentration of surface benzyl species over pure ZrO_2 (O_2-toluene feed ratio: 1.1 × theoretical toluene total oxidation ratio, heating rate: 10 °C/min).

their common surface precursor. A better fit was however obtained with separate surface-catalyzed oxidation kinetics.

3.4. Discussion

The aim of the kinetic modeling was to obtain a reaction mechanism for toluene oxidation over ZrO_2-based catalysts. In addition to the molar flow of toluene, all the other measured molar flows were fitted in the modeling. Since ZrO_2-based catalysts oxidize toluene into four products [9], the reaction mechanism derived in this work should be able to predict the formation of all products, including the incomplete oxidation products, i.e., CO and H_2. A schematic presentation of the model is shown in Fig. 7.

The first reaction in the toluene oxidation model is the adsorption of toluene as a surface benzyl species over ZrO_2-based catalysts (Reaction (R1)). The data analysis on the formation and consumption of C, O and H atoms (Fig. 3) as well as our previous spectroscopic results [8] clearly supported this assumption. Furthermore, over several other oxide catalysts, the formation of benzyl species from toluene has been suggested to be the first step in both selective oxidation [34] and total oxidation of toluene [35] as well as in toluene ammoxidation [36]. Also quantum-chemical calculations on vanadium-based catalysts have shown that side-on adsorption of toluene leads to the complete destruction of the aromatic ring and formation of coke or carbon oxides [37].

The kinetic models suggested in the VOC literature for toluene oxidation/combustion rarely include the formation of the surface benzyl species as the first step. Most of the published kinetic models for toluene total oxidation are based on the simplest power-law rate model or on different mechanistic assumptions. For example, Langmuir-Hinshelwood type models have been used to describe toluene oxidation over $Cu_{0.13}Ce_{0.87}O_y$ catalysts [11], over Pd/mesoporous carbon [31] and over $Cu_{1.5}Mn_{1.5}O_4$ [32]. The Mars and van Krevelen model has been used as well to describe toluene oxidation over Pt/Al_2O_3 [38] and over pure ZrO_2 (in a study of Mo oxides on different supports) [30]. All of the abovementioned models described the consumption of toluene rather well but the rates of experimental and calculated product formations were not fitted in any of these publications.

More detailed toluene total oxidation models have been suggested by Menon et al. [39] and by Rezaei and Soltan [40]. In the model by Menon et al. [39] based on the Mars and van Krevelen mechanism, the catalytic total oxidation of toluene goes through several steps over CuO—CeO_2/Al_2O_3 catalyst. In the first step toluene is adsorbed flat on the catalyst surface with the aromatic ring on Cu^{2+} and the methyl group on O^{2-} [39]. Thus, the formation of surface benzyl species from toluene adsorption is not considered in their model. Furthermore, the experimental and calculated molar flows of only toluene, oxygen and CO_2 were fitted [39]. In the model by Rezaei and Soltan [40] the formation of the benzyl species is considered as the first step in the catalytic oxidation of toluene by ozone over MnO_x/γ-alumina. Their model is based on the Langmuir-Hinshelwood formalism. However, neither the fits of toluene nor the products of the model suggested by Rezaei and Soltan [40] have been published.

The H atom abstracted from toluene upon the formation of benzyl species has been suggested to form water with adsorbed oxygen atoms [40] or to form an OH group on the catalyst surface [41]. Actually, the formation of gas-phase hydrogen has not been detected, measured and/or reported in any other toluene oxidation studies. The hydrogen abstracted upon benzyl formation seems to end up in the pool to form gas phase H_2, together with that evolved from the [C_3H_3] fragment resulting from the decomposition of benzyl species.

The products follow pairwise synchronized dynamics (Fig. 4), implying a common surface intermediate for CO_2 and water formation and one for CO and H_2 formation. In the model, the surface

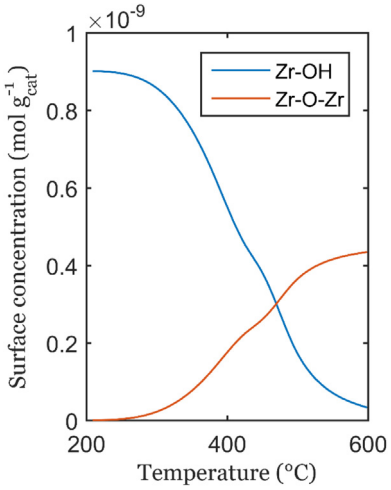

Fig. 9. Calculated concentrations of Zr-OH and Zr-O-Zr surface sites over pure ZrO_2 (O_2-toluene feed ratio: 1.1 × theoretical toluene total oxidation ratio, heating rate: 10 °C/min).

benzyl species are directly oxidized in one net reaction (Reaction (R2)) into four products. Simulated surface concentration of the benzyl species is shown in Fig. 8. The maximum surface concentration of benzyl species was at 400 °C, in agreement with our previous spectroscopic results [8].

The direct oxidation of the surface benzyl species in one single net Reaction (R2) can be broken down into several surface reactions (R2a–d in Fig. 7). All of the obtained product ratios can be achieved when seven carbon atoms of the benzyl species react so that 4 CO_2 molecules and 3 CO molecules are formed. Therefore, it is suggested that the benzyl species disassembles into a $[C_4H_4]$ fragment and a $[C_3H_3]$ fragment according to Reaction (R7).

$$[C_7H_7] \rightarrow [C_4H_4] + [C_3H_3] \quad \text{(R7)}$$

These two fragments of the benzyl species then react differently; one is oxidized into CO_2 and H_2O, whereas the other into CO and H_2. In order to meet the obtained CO_2/CO ratio, the $[C_4H_4]$ fragment is oxidized into CO_2 and H_2O (Reaction (R8)) and the $[C_3H_3]$ fragment into CO and H_2 (Reaction (R9)).

$$[C_4H_4] + 5O_2(g) \rightarrow 4CO_2(g) + 2H_2O(g) \quad \text{(R8)}$$

$$[C_3H_3] + 1.5O_2(g) \rightarrow 3CO(g) + 1.5H_2(g) \quad \text{(R9)}$$

We propose that activated toluene (surface benzyl species) decomposes rapidly into two extremely short-lived fragments containing four carbon and four hydrogen atoms and three carbon and three hydrogen atoms, respectively. The first fragment leads directly to $4CO_2 + 2H_2O$, whereas the other fragment together with the fourth hydrogen atom available from benzyl formation forms predominantly $3CO + 2H_2$. The latter fragment may also form $3CO_2 + 2H_2O$ under excess oxygen at high temperatures. These stoichiometries for the proposed surface species and their decomposition reactions follow directly from the gas phase analysis over versatile temperatures and conversion levels and from the conservation of atoms in chemical reactions.

The benzyl species is assumed to be attached to a surface Zr cation by its benzene ring and to a surface OH group from its methylene group ($-CH_2$). Keeping in mind that neither benzene nor benzene derivatives were detected, the C—C bond between the aromatic ring and the methylene group is not suggested to break at this point. Instead, the carbon atom of the methylene group and its neighboring carbon atom in the aromatic ring are withdrawn towards the OH group of the catalyst, thus weakening the next aromatic C—C bonds. Therefore, it is suggested that two carbon atoms of the aromatic ring and the methylene group, i.e., the $[C_3H_3]$ fragment, could follow the oxidation Reaction (R9) into incomplete oxidation products. The remaining four carbon and four hydrogen atoms ($[C_4H_4]$ fragment) of the aromatic ring attached to the Zr cation are considered to have equal bond strengths and to be oxidized according to Reaction (R8).

As the identity of these fragments cannot be spectroscopically verified owing to their supposedly short lifetime over the catalyst surface, we propose identities based on their atomic compositions. Three-carbon containing surface species could be tentatively surface acrolein (propenal, C_3H_4O) and four-carbon containing fragment could be surface furan (C_4H_4O). The oxygen in these short-lived surface oxygenates is proposed to be either lattice oxygen of zirconia or more labile adsorbed oxygen originating from the gas-phase O_2. The activation of toluene into benzyl appears to require adsorbed oxygen, as this species forms only in the presence of gas phase O_2 according to our previous spectroscopic findings [8].

The steps that follow the adsorption of toluene suggested in the literature differ greatly from those proposed in the present work. In the toluene oxidation model by Menon et al. [10,39], the steps following the adsorption of toluene are the abstractions of H atoms from the methyl and phenyl groups of toluene. Similarly in the model proposed by Rezaei and Soltan [40], the surface benzyl species undergoes multiple H abstractions leaving a hydrogen-free carbon structure. In both cases, the abstracted H atoms react with adsorbed or lattice oxygen, producing water that desorbs from the catalyst surface [10,40]. In the model by Menon et al. [10,39], the carbon atom originating from the methyl group is then separated from the aromatic ring followed by the breakage of remaining C—C bonds. Next, the C—O bond containing intermediates are formed when C atoms react with lattice/surface oxygen and finally CO_2 is formed when these intermediates are further oxidized with lattice/surface oxygen [10,39]. Likewise in the model by Rezaei and Soltan [40], the remaining carbon structure reacts with adsorbed oxygen atoms to produce CO and CO_2.

Oxidation of hydrocarbons over transition metal oxide catalysts usually occurs according to the Mars and van Krevelen mechanism, where oxidation of the reactant takes place using lattice oxygen, which is then replaced by oxygen from the gas phase [42]. This is not in an agreement with our observations of toluene oxidation on zirconia. Therefore, the compiled model does not include the adsorption of gas phase oxygen, dissociation of oxygen nor the oxidation of surface species using adsorbed oxygen. Oxygen is not believed to dissociate at as low as 350 °C on zirconia. That is implied by the results of Foraita et al. [43] where temperature-programmed isotopic exchange of oxygen shows that oxygen is able to dissociate above 460 °C on monoclinic and above 500 °C on tetragonal zirconia. We believe that benzyl species is stabilized together with a superoxide surface species (O_2^-). This kind of combined hydrocarbon and superoxide surface species has been verified on several oxides including zirconia [44]. It is in agreement with our observation that benzyl species, which was detected with DRIFTS, could be formed only in the presence of gas-phase oxygen [8]. On the other hand, precalcined zirconia could not oxidize toluene at all without the presence of gas-phase oxygen ruling out the conventional Mars and van Krevelen oxidation mechanism. When the superoxide–benzyl surface complex becomes unstable, the reaction probably proceeds via instant radical mechanism leading to fragments of constant composition and their subsequent oxidation with the gas-phase oxygen. This is in line with the spectroscopic observation that no intermediate surface species following the benzyl could be detected [8] and only the reported four gas-phase products evolved when toluene oxidation took place. However, associative adsorption of oxygen was tested to be included in the model but the fit of the model did not improve. Furthermore, the activation energy of Reaction (R2) increased to a physically mean-

ingless level. For these reasons, the benzyl species (or its fragments) are believed to be oxidized using superoxide surface species (O_2^-) over ZrO_2-based catalysts.

In the derived model, the secondary reactions have been suggested to be the surface-catalyzed oxidation of CO (Reaction (R3)) and that of H_2 (Reaction (R4)). The oxidation activity of CO in the temperature range of 300–600 °C over ZrO_2-based catalysts has been reported in Part A [9]. Thus, it is believed to be a secondary reaction in toluene oxidation. It was also proposed in the model by Rezaei and Soltan [40] that the hydrogen-free aromatic ring was first oxidized into CO, and then either desorbed from the catalyst or further oxidized into CO_2. The oxidation of H_2 was suggested to be a secondary reaction in our model based on the evident shape similarity with CO formation. Both of these secondary reactions describe the experimental data very well. The activation energies obtained for CO and H_2 oxidation reactions were 97 and 113 kJ/mol, respectively (see Table 2).

The dehydroxylation (Reaction (R5)) and the hydroxylation (Reaction (R6)) of the ZrO_2 surface were included in the derived model. The activation energy of dehydroxylation was around 100 kJ/mol, whereas hydroxylation was inactivated (Table 2). The concentrations of Zr-OH and the Zr-O-Zr sites are shown in Fig. 9. The amount of Zr-OH sites decreased with increasing temperature, while the amount of Zr-O-Zr surface sites increased with temperature throughout the studied temperature range. The initial amounts available for toluene oxidation of Zr-OH and Zr-O-Zr surface sites were also simulated and it seems that in the beginning of the experiment only Zr-OH surface sites are available for toluene oxidation.

The rate determining step of our toluene oxidation model is assumed to be the oxidation of the surface benzyl species into the products. This rate limiting step is in good agreement with toluene (amm)oxidation kinetic study of Sanati and Andersson [36] over supported vanadia catalysts. They showed that abstraction of hydrogen from toluene upon the formation of benzyl species is not rate limiting but rather the following step, i.e., the interaction of surface benzyl species with surface oxide species [36]. Also Menon et al. [39] suggested that the potentially slowest step is the destruction of the aromatic ring.

Toluene oxidation model developed over ZrO_2 was also fitted against the data collected over Y_2O_3-ZrO_2 (Fig. S3 in the Supplementary data) and SiO_2-ZrO_2 (Fig. S4 in the Supplementary data) without dehydroxylation and hydroxylation reactions. The model (consisting of Reactions from (R1) to (R4)) was able to produce most of the curve shapes over these catalysts as well. Over Y_2O_3-ZrO_2 (Fig. S3 in the Supplementary data), the model deviated slightly from the measured CO_2 molar flows in the temperature range of 300–400 °C. However, this deviation could be explained by CO_2 desorption from the catalyst surface. It is possible that the redox surface sites of Y_2O_3-ZrO_2 could have oxidized some toluene molecules already at 200 °C (before the beginning of the ramp) and, thus, showing desorption of these CO_2 molecules at 300–400 °C. This is supported by the observed desorption of preadsorbed CO_2 from this catalyst at temperatures below 400 °C [7]. The model underestimates also the formation of water between 350 and 550 °C. Water desorption from reduced (at 400 °C) and evacuated (at room temperature) surface of Y_2O_3-ZrO_2 has been reported to have maxima at 427 °C by Kogler et al. [27]. Thus, it can be suggested that in toluene oxidation experiments, the formation of water at 350–550 °C is due to the water desorption from the surface of Y_2O_3-ZrO_2 as well as from toluene oxidation as a product. As over pure ZrO_2, the model is not fully capable of reproducing the maxima of the CO curves. Slight deviation is also observed between 300 and 400 °C in the experimental and calculated CO molar flows. Similar to CO_2 desorption from the surface, CO desorption could have taken place as well. Over SiO_2-ZrO_2 (Fig. S4 in the Supplementary data), the deviation of experimental and calculated values was much higher than over Y_2O_3-ZrO_2. However, toluene curve was fitted rather nicely also over SiO_2-ZrO_2. In addition, the model was able to reproduce most of the shapes of the other curves (oxygen and product curves) but the maxima of these curves was severely underestimated. The estimated parameters for the doped zirconias are only preliminary and therefore are not reported.

4. Conclusions

Toluene oxidation over ZrO_2, Y_2O_3-ZrO_2 and SiO_2-ZrO_2 was studied in temperature-programmed mode in the range of 200 °C to 600 °C. The multiresponse dynamic reaction data on two reactants (toluene and oxygen) and four products (CO_2, H_2O, CO and H_2) were subjected to transient kinetic modeling. A thorough qualitative data analysis preceded the mathematical modeling. The formation of products started slightly later than the toluene consumption, suggesting that an intermediate surface species (benzyl) was formed. Next, the surface benzyl species underwent a rapid and simultaneous decomposition into four products. The product curves showed dynamic similarities in the pairs of CO_2 & H_2O and CO & H_2. For a range of conditions, all the products were primary toluene decomposition products, while only close to the conditions of complete conversion of toluene the formed CO and H_2 started to oxidize further. Zirconia catalysts were proven to manifest exceptional performance in preferential toluene oxidation. The present study demonstrates the applicability of temperature programming as a transient technique for comprehensive mechanistic investigations, kinetic model development and parameter estimation.

Acknowledgements

The authors thank Ms. Heidi Meriö-Talvio for assistance with the experiments. The authors gratefully acknowledge the financial support of the Ministry of Education of Finland and the Academy of Finland. The zirconia samples were kindly provided by MEL Chemicals.

Appendix A. Supplementary data

Supplementary data associated with this article can be found, in the online version, at http://dx.doi.org/10.1016/j.apcatb.2016.06.015.

References

[1] P. Gallezot, A. Kiennemann, Conversion of biomass on solid catalysts, in: G. Ertl, H. Knözinger, F. Schüth, J. Weitkamp (Eds.), Handbook of Heterogeneous Catalysis, Wiley-VCH Weinheim, 2008.
[2] D. Sutton, B. Kelleher, J.R.H. Ross, Review of literature on catalysts for biomass gasification, Fuel Process. Technol. 155 (2001), http://dx.doi.org/10.1016/S0378-3820(01)00208-9.
[3] P. Simell, E. Kurkela, P. Ståhlberg, J. Hepola, Catalytic hot gas cleaning of gasification gas, Catal. Today 27 (1996) 55–62, http://dx.doi.org/10.1016/0920-5861(95)00172-7.
[4] W. Torres, S.S. Pansare, J.G. Goodwin, Hot gas removal of tars, ammonia, and hydrogen sulfide from biomass gasification gas, Catal. Rev. 49 (2007) 407–456, http://dx.doi.org/10.1080/01614940701375134.
[5] H. Rönkkönen, P. Simell, A.O.I. Krause, The effect of sulfur on ZrO_2-based biomass gasification gas clean-up catalysts, Top. Catal. 52 (2009) 1070.
[6] S.J. Juutilainen, P.A. Simell, A.O.I. Krause, Zirconia: selective oxidation catalyst for removal of tar and ammonia from biomass gasification gas, Appl. Catal. B Environ. 62 (2006) 86–92, http://dx.doi.org/10.1016/j.apcatb.2005.05.009.
[7] T. Viinikainen, H. Rönkkönen, H. Bradshaw, H. Stephenson, S. Airaksinen, M. Reinikainen, et al., Acidic and basic surface sites of zirconia-based biomass gasification gas clean-up catalysts, Appl. Catal. A Gen. 362 (2009) 169–177.
[8] T. Viinikainen, I. Kauppi, S. Korhonen, L. Lefferts, J. Kanervo, J. Lehtonen, Molecular level insights to the interaction of toluene with ZrO_2-based biomass gasification gas clean-up catalysts, Appl. Catal. B Environ. 142–143 (2013) 769–779.
[9] T. Viinikainen, S. Kouva, J. Lehtonen, J. Kanervo, Toluene oxidation over ZrO_2-based gasification gas clean-up catalysts: Part A. Effect of oxygen and

temperature on the product distribution, Appl. Catal. B Environ. (2016), http://dx.doi.org/10.1016/j.apcatb.2016.06.014.
[10] U. Menon, V.V. Galvita, G.B. Marin, Reaction network for the total oxidation of toluene over CuO–CeO_2/Al_2O_3, J. Catal. 283 (2011) 1–9, http://dx.doi.org/10.1016/j.jcat.2011.05.024.
[11] C. Hu, Catalytic combustion kinetics of acetone and toluene over $Cu_{0.13}Ce_{0.87}O_y$ catalyst, Chem. Eng. J. 168 (2011) 1185–1192, http://dx.doi.org/10.1016/j.cej.2011.02.006.
[12] J.J. Spivey, Complete catalytic oxidation of volatile organics, Ind. Eng. Chem. Res. 26 (1987) 2165.
[13] J.M. Kanervo, K.M. Reinikainen, A.O.I. Krause, Kinetic analysis of temperature-programmed desorption, Appl. Catal. A Gen. 258 (2004) 135–144.
[14] F. Arena, F. Frusteri, A. Parmaliana, N. Giordano, Temperature-programmed reaction: a powerful and reliable method for catalyst testing in the partial oxidation of methane to formaldehyde, Appl. Catal. A Gen. 125 (1995) 39–59, http://dx.doi.org/10.1016/0926-860X(94)00232-0.
[15] R.J. Berger, F. Kapteijn, J.A. Moulijn, G.B. Marin, J. De Wilde, M. Olea, et al., Dynamic methods for catalytic kinetics, Appl. Catal. A Gen. 342 (2008) 3–28, http://dx.doi.org/10.1016/j.apcata.2008.03.020.
[16] T. Finke, M. Gernsbeck, U. Eisele, C. Vincent, M. Hartmann, S. Kureti, et al., Numerical modelling of the adsorption and thermal desorption of NH3 on ZrO2, Thermochim. Acta 473 (2008) 32–39, http://dx.doi.org/10.1016/j.tca.2008.04.006.
[17] J.M. Kanervo, A.O.I. Krause, H_2-TPR kinetics; case study on the reduction of a CrO_x/Al_2O_3 catalyst, in: Studies in Surface Science Catalysis, Elsevier, 2001, pp. 593–598, http://dx.doi.org/10.1016/S0167-2991(01)82017-6.
[18] P. Heidebrecht, V. Galvita, K. Sundmacher, An alternative method for parameter identification from temperature programmed reduction (TPR) data, Model. Exp. Anal. 63 (2008) 4776–4788, http://dx.doi.org/10.1016/j.ces.2007.10.012.
[19] T.J. Keskitalo, K.J.T. Lipiäinen, A.O.I. Krause, Kinetic modeling of coke oxidation of a ferrierite catalyst, Ind. Eng. Chem. Res. 45 (2006) 6458, http://dx.doi.org/10.1021/ie060521g.
[20] S. Wagloehner, S. Kureti, Modelling of the kinetics of the catalytic soot oxidation on Fe_2O_3, Appl. Catal. B Environ. 129 (2013) 501–508, http://dx.doi.org/10.1016/j.apcatb.2012.09.055.
[21] E.I. Kauppi, E.H. Rönkkönen, S.M.K. Airaksinen, S.B. Rasmussen, M.A. Bañares, A.O.I. Krause, Influence of H_2S on ZrO_2-based gasification gas clean-up catalysts: MeOH temperature-programmed reaction study, Appl. Catal. B Environ. 111–112 (2012) 605–613, http://dx.doi.org/10.1016/j.apcatb.2011.11.013.
[22] J.M. Kanervo, T.J. Keskitalo, R.I. Slioor, A.O.I. Krause, Temperature-programmed desorption as a tool to extract quantitative kinetic or energetic information for porous catalysts, J. Catal. 238 (2006) 382–393, http://dx.doi.org/10.1016/j.jcat.2005.12.026.
[23] J. D'Errico, FMINSEARHCBND, 2012. http://www.mathworks.com/matlabcentral/fileexchange/8277-fminsearchbnd-fminsearchcon.
[24] D.A.M. Monti, A. Baiker, Temperature-programmed reduction Parametric sensitivity and estimation of kinetic parameters, J. Catal. 83 (1983) 323–335, http://dx.doi.org/10.1016/0021-9517(83)90058-1.
[25] J. Zhu, M.S.M.M. Rahuman, J.G. van Ommen, L. Lefferts, Dual catalyst bed concept for catalytic partial oxidation of methane to synthesis gas, Appl. Catal. A Gen. 259 (2004) 95–100, http://dx.doi.org/10.1016/j.apcata.2003.09.022.
[26] S. Schmidt, S. Giesa, A. Drochmer, H. Vogel, Catalytic tar removal from bio syngas—catalyst development and kinetic studies, Catal. Today 175 (2011) 442, http://dx.doi.org/10.1016/j.cattod.2011.04.052.
[27] M. Kogler, E.M. Köck, T. Bielz, K. Pfaller, B. Klötzer, D. Schmidmair, et al., Hydrogen surface reactions and adsorption studied on Y_2O_3, YSZ, and ZrO_2, J. Phys. Chem. C 118 (2014) 8435–8444, http://dx.doi.org/10.1021/jp5008472.
[28] D. Bianchi, T. Chafik, M. Khalfallah, S.J. Teichner, Intermediate species on zirconia supported methanol aerogel catalysts V. Adsorption of methanol, Appl. Catal. A Gen. 123 (1995) 89–110, http://dx.doi.org/10.1016/0926-860X(94)00242-8.
[29] S. Kouva, J. Andersin, K. Honkala, J. Lehtonen, L. Lefferts, J. Kanervo, Water and carbon oxides on monoclinic zirconia: experimental and computational insights, Phys. Chem. Chem. Phys. 16 (2014) 20650–20664, http://dx.doi.org/10.1039/C4CP02742F.
[30] N.K. Nag, T. Fransen, P. Mars, The oxidation of toluene on various molybdenum-containing catalysts, J. Catal. 68 (1981) 77–85, http://dx.doi.org/10.1016/0021-9517(81)90041-5.
[31] J. Bedia, J.M. Rosas, J. Rodríguez-Mirasol, T. Cordero, Pd supported on mesoporous activated carbons with high oxidation resistance as catalysts for toluene oxidation, Appl. Catal. B Environ. 94 (2010) 8–18, http://dx.doi.org/10.1016/j.apcatb.2009.10.015.
[32] S. Behar, N.-A. Gómez-Mendoza, M.-Á. Gómez-García, D. Świerczyński, F. Quignard, N. Tanchoux, Study and modelling of kinetics of the oxidation of VOC catalyzed by nanosized Cu–Mn spinels prepared via an alginate route, Appl. Catal. A Gen. 504 (2014) 203–210, http://dx.doi.org/10.1016/j.apcata.2014.12.021.
[33] Lazarova Markova-Velichkova, Ivanov Tumbalev, Stefanov Kovacheva, et al., Complete oxidation of hydrocarbons on $YFeO_3$ and $LaFeO_3$ catalysts, Chem. Eng. J. 231 (2013) 236–244, http://dx.doi.org/10.1016/j.cej.2013.07.029.
[34] G. Busca, Infrared characterization of the hydrocarbon intermediates in the oxidation of toluene and xylenes over vanadia-titania catalysts, J. Chem. Soc. Faraday Trans. 89 (1993) 753, http://dx.doi.org/10.1039/ft9938900753.
[35] G. Busca, T. Zerlia, V. Lorenzelli, A. Girelli, Fourier transform-infrared study of the adsorption of unsaturated and aromatic hydrocarbons on the surface of a-Fe_2O_3. Part III. Toluene, ethylbenzene and styrene, React. Kinet. Catal. Lett. 27 (1985) 429–432, http://dx.doi.org/10.1007/BF02070488.
[36] S. Mehri, A. Andersson, Kinetics and mechanisms in the ammoxidation of toluene over a TiO_2(B) – supported vanadium oxide monolayer catalyst. 1. Selective reactions, Ind. Eng. Chem. Res. 30 (1991) 312–320.
[37] J. Haber, M. Witko, Quantum-chemical modelling of hydrocarbon oxidation on vanadium-based catalysts, Catal. Today 23 (1995) 311–316, http://dx.doi.org/10.1016/0920-5861(94)00143-P.
[38] S. Ordóñez, L. Bello, H. Sastre, R. Rosal, F.V. Díez, Kinetics of the deep oxidation of benzene, toluene, n-hexane and their binary mixtures over a platinum on γ-alumina catalyst, Appl. Catal. B Environ. 38 (2002) 139–149, http://dx.doi.org/10.1016/S0926-3373(02)00036-X.
[39] U. Menon, V.V. Galvita, D. Constales, K. Alexopoulos, G. Yablonsky, G.B. Marin, Microkinetics for toluene total oxidation over CuO–CeO_2/Al_2O_3, Catal. Today 258 (2015) 214–224, http://dx.doi.org/10.1016/j.cattod.2015.07.015.
[40] E. Rezaei, J. Soltan, EXAFS and kinetic study of MnO_x/γ-alumina in gas phase catalytic oxidation of toluene by ozone, Appl. Catal. B Environ. 148–149 (2014) 70–79, http://dx.doi.org/10.1016/j.apcatb.2013.10.041.
[41] S.L.T. Andersson, Reaction networks in the catalytic vapor-phase oxidation of toluene and xylenes, J. Catal. 98 (1986) 138–149, http://dx.doi.org/10.1016/0021-9517(86)90304-0.
[42] P. Mars, D.W. van Krevelen, Oxidations carried out by means of vanadium oxide catalysts, Chem. Eng. Sci. 3 (1954) 41–59, http://dx.doi.org/10.1016/S0009-2509(54)80005-4.
[43] S. Foraita, J.L. Fulton, Z.A. Chase, A. Vjunov, P. Xu, E. Baráth, et al., Impact of the oxygen defects and the hydrogen concentration on the surface of tetragonal and monoclinic ZrO_2 on the reduction rates of stearic acid on Ni/ZrO_2, Chemistry 21 (2015) 2423–2434, http://dx.doi.org/10.1002/chem.201405312.
[44] A.F. Bedilo, M.A. Plotnikov, N.V. Mezentseva, A.M. Volodin, G.M. Zhidomirov, I.M. Rybkin, et al., Superoxide radical anions on the surface of zirconia and sulfated zirconia: formation mechanisms, properties and structure, Phys. Chem. Chem. Phys. 7 (2005) 3059–3069, http://dx.doi.org/10.1039/b504262c.